Nuclear Inst. and Methods in Physics Research, A 900 (2018) 60–63

Contents lists available at ScienceDirect

Nuclear Inst. and Methods in Physics Research, A

journal homepage: www.elsevier.com/locate/nima

Measuring low-energy (α, p) reaction cross sections using an extended gas target and gas recirculator

K.Y. Chae [a,*], S. Ahn [b], A. Ayres [b], D.W. Bardayan [c], A. Bey [b], U. Greife [d], M.E. Howard [e], K.L. Jones [b], R.L. Kozub [f], M. Matoš [g], B.H. Moazen [g], C.D. Nesaraja [h], P.D. O'Malley [e], W.A. Peters [i], S.T. Pittman [b], M.S. Smith [h]

[a] Department of Physics, Sungkyunkwan University, Suwon 16419, Republic of Korea
[b] Department of Physics and Astronomy, University of Tennessee, Knoxville, TN 37996, USA
[c] Department of Physics, University of Notre Dame, Notre Dame, IN 46556, USA
[d] Colorado School of Mines, Golden, CO 80401, USA
[e] Department of Physics and Astronomy, Rutgers University, Piscataway, NJ 08854, USA
[f] Department of Physics, Tennessee Technological University, Cookeville, TN 38505, USA
[g] Department of Physics and Astronomy, Louisiana State University, Baton Rouge, Loisiana 70803, USA
[h] Physics Division, Oak Ridge National Laboratory, Oak Ridge, TN 37831, USA
[i] Oak Ridge Associated Universities, Oak Ridge, TN 37831, USA

ARTICLE INFO

Keywords:
Extended gas target
$^{19}F(\alpha, p)^{22}Ne$ reaction
Inverse kinematics
αp-process
Heavy ion beam

ABSTRACT

Direct measurements of (α, p) reactions of astrophysical interest with radioactive beams presents serious challenges because of the difficult nature of helium targets and the typical low intensities of the beams. To address this, a new technique has been developed for measurements of low-energy (α, p) reactions with heavy ion beams using an extended ^{4}He gas target and a newly developed gas recirculating system. The system was used to measure the $^4He(^{19}F, ^1H)^{22}Ne$ reaction as a demonstration. Excitation functions of the $^{19}F(\alpha, p)^{22}Ne$ and $^{19}F(\alpha, p')^{22}Ne^*$ reactions were successfully measured to show the viability of this technique. Details of the approach and future plans are given.

1. Introduction

The αp-process, which consists of a series of alternating (α, p) and (p, γ) reactions, plays a crucial role in understanding the synthesis of heavy elements in X-ray bursts [1,2]. The process provides a bridge between reactions in the CNO cycle and those in the rp-process which synthesizes heavy elements up to the Sn–Sb–Te region within an outburst lasting ~10 s [3]. Most of the important (α, p) reactions, however, have never been experimentally determined in the laboratory because of the need for radioactive heavy ion beams bombarding helium targets in inverse kinematics.

There are only a few previous direct measurements of such (α, p) reactions with radioactive heavy ion beams [4–7]. These studies, however, utilized ^{4}He gas cell targets with thick solid windows containing the gas. For instance, a 2.0 mg/cm^2-thick nickel foil was used to confine 500 mbar (~375 Torr) ^{4}He gas in the reaction target chamber in Ref. [4]. At the low beam energies relevant for astrophysical (α, p) reactions, this causes significant energy loss and straggling of the beam particles, seriously degrading the energy resolution of the measurement. Moreover, the events of interest are difficult to distinguish from high background rates produced by reactions on the windows. To avoid these types of backgrounds and to provide the necessary sensitivities, improved techniques need to be developed to study (α, p) reactions with radioactive beams. In recent α scattering measurements performed in inverse kinematics, a very large thick target method was used to circumvent the problems [8,9]. In our approach, a heavy ion beam impinges on a windowless pure gas target, enabling high sensitivities for measurements with radioactive ion beams.

Our novel technique is based on using a differentially pumped windowless gas target [10]. The approach was first used with H_2 gas to study the properties of the 183 keV resonance in the $^{17}O(p, \alpha)^{14}N$ reaction which is important for understanding nucleosynthesis in giant stars and nova explosions. With hydrogen gas at pressures up to 4 Torr, this approach was proven to be very useful for the measurement of narrow resonances in (p, α) reactions: the resonance energy, resonance strength,

* Corresponding author.
E-mail address: kchae@skku.edu (K.Y. Chae).

https://doi.org/10.1016/j.nima.2018.05.053
Received 3 April 2018; Received in revised form 19 May 2018; Accepted 24 May 2018
Available online 28 May 2018

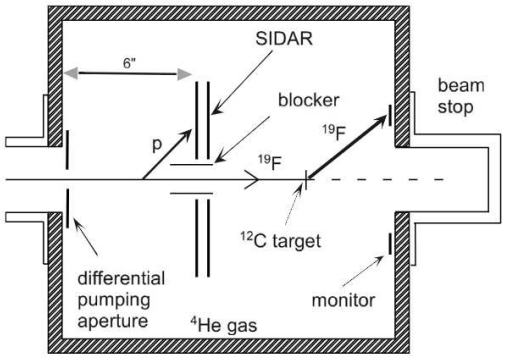

Fig. 1. A schematic diagram of the experimental setup is shown. Recoiling protons from the reaction were detected by an annular silicon strip detector array which was configured in a $\Delta E-E$ telescope mode. The unreacted ^{19}F beam particles passed through the center of the array and impinged on a 50 μg/cm^2-thick carbon foil for beam current normalization. See text for more details.

and the upper limit on the total width of the level of interest were precisely determined. In the present work, this approach was extended to helium gas and combined with a newly developed gas recirculation system to measure the ^{19}F$(\alpha,p)^{22}$Ne reaction in inverse kinematics. The reaction was chosen since it has been previously measured [11–13] with α beams.

2. Experimental setup

The ^{19}F$(\alpha,p)^{22}$Ne reaction was measured at the Holifield Radioactive Ion Beam Facility (HRIBF) at Oak Ridge National Laboratory (ORNL) [14] in inverse kinematics by bombarding low-energy beams of ^{19}F from the HRIBF tandem accelerator with an typical intensity of ~300 epA on a large scattering chamber filled with ^{4}He gas at pressures of up to 9 Torr. A schematic illustration of the experimental setup is shown in Fig. 1. The gas in the chamber served as a spatially extended target for the (α,p) reaction. The gas pressure at the reaction target chamber was continuously monitored by using a MKS absolute capacitance Baratron manometer rated to 1 mTorr accuracy. The pressure was regulated to better than ±3% during the runs. A vacuum of $\sim10^{-6}$ Torr upstream of the chamber could be achieved by employing the differential pumping system which was originally designed for a windowless gas target system developed at HRIBF for capture reaction measurements [15] and was later modified for use with a large silicon detector array in the gas [10].

A collimating aperture with a 5 mm diameter hole was used at the entrance of the reaction target chamber as a differential pumping aperture for the ^{4}He gas (Fig. 1). This aperture was sufficiently wide to pass the ~ few mm wide beams typically produced by the HRIBF tandem. Four differentially pumped chambers were used to pump out residual gas upstream of the target as described in Ref. [10]. Roots mechanical pumps were used at the first differential pumping stage, which is located just upstream of the target chamber, in order to reduce the pressure to few tens of mTorr. The pressure was then further reduced at the other stages of the pumping system by using turbomolecular pumps. The beamline pressure of $\sim10^{-6}$ Torr could be achieved within ~30 cm by this differential pumping system.

The collected ^{4}He gas molecules at various pumping stages were injected into a newly built gas recirculator (Fig. 2) to be purified and sent back into the reaction target chamber. The recirculator was developed to reduce the gas usage when light gas molecules such as hydrogen and helium are used at the extended gas target system. Both left and right sections of the recirculator are composed of three manual valves ("in", "out", and "to vacuum") and a zeolite filter as shown in the figure. The "to vacuum" valves are used to open one section of the recirculator to the regenerator pump, an Ebara A10S multi-stage dry pump. One side of the system can be isolated from the other, which allows the continuous using of one side for gas recirculation while the other side is being regenerated. A residual gas analyzer was used to check the purity of the ^{4}He gas, with values typically greater than 99.99% during a run of 3–4 h. The gas volume was flushed between the runs to ensure the highest level purity.

Recoiling protons from the ^{4}He$(^{19}$F,^{1}H$)^{22}$Ne reaction populating both the ground and first excited ^{22}Ne states were detected with a large area annular silicon strip detector array, SIDAR [16]. By combining thin (100 μm-thick, ΔE) and thick (1000 μm-thick, E) detectors, SIDAR was configured in a ΔE-E telescope mode for particle identification. SIDAR was placed approximately 152 mm from the entrance of the chamber. To block the majority of elastically scattered α particles at large angles ($\theta_{\rm lab} > 70°$, $\theta_{\rm c.m.} < 40°$), a hollow cylinder (Fig. 1) was installed at the center of the array. The unreacted ^{19}F beam particles passed through the center of the array and impinged on a 50 μg/cm^2-thick carbon foil before striking the beam stop. Some ^{19}F particles were scattered off the carbon target and detected with two silicon surface barrier detectors mounted at the end of the target chamber for the beam current normalization.

3. Data analysis and results

The ^{19}F$(\alpha,p)^{22}$Ne and ^{19}F$(\alpha,p')^{22}$Ne* reactions were studied using ^{19}F beams at 20 different beam energies ranging over $E_{\rm beam}$ =

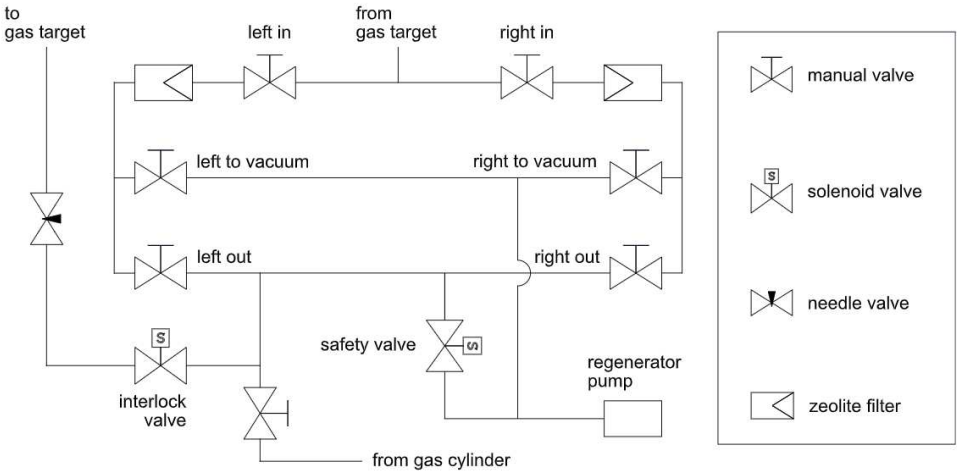

Fig. 2. The schematic of the gas recirculating system is shown.

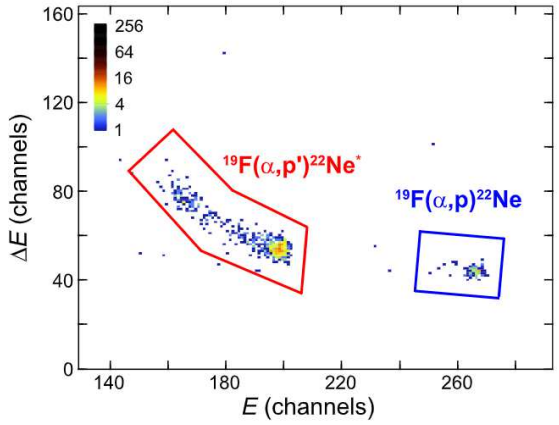

Fig. 3. (Color online) A typical particle identification plot obtained from a ΔE-E telescope is shown. The events falling in the blue and red gates were identified as protons from the (α, p) and (α, p') reactions, respectively. The range of ΔE in each gate arises from the range of reaction angles included. The beam energy was 12 MeV. (For interpretation of the references to color in this figure legend, the reader is referred to the web version of this article.)

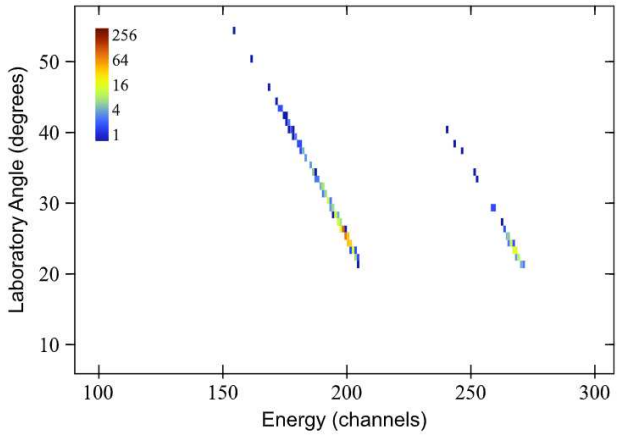

Fig. 4. (Color online) The reconstructed angle versus energy plot obtained at $E_{\text{beam}} = 12$ MeV is shown. The right and left curves represent the events from the (α, p) and (α, p') channel of the reaction, respectively.

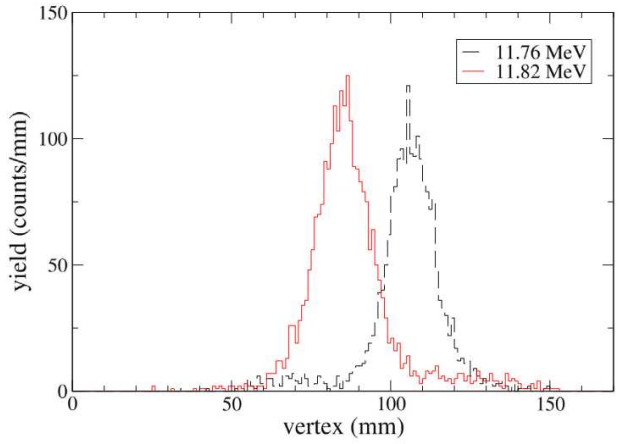

Fig. 5. (Color online) The reaction yield versus the distance from the reaction vertex to the plane of SIDAR plot is shown for $E_{\text{beam}} = 11.76$ MeV (dotted black curve) and 11.82 MeV (solid red curve) for the (α, p') channel.

11.55–12.12 MeV. Protons from the (α, p) and (α, p') reactions were identified by the SIDAR. A typical particle identification plot is shown in Fig. 3. The events falling in the blue and red gates were identified as protons from the (α, p) and (α, p') reactions, respectively. A state in the compound nucleus ^{23}Na (the ^{19}F + α system) can decay into the ground state of the ^{22}Ne nucleus via the (α, p) channel or the first excited state at $E_x = 1.274$ MeV via the (α, p') channel. Two reaction channels are clearly separated in the particle identification plot (Fig. 3) owing to different reaction Q-values.

The total energy of each event in the proton gate was reconstructed by summing the energies deposited in the ΔE and E layers of the silicon detector array. The energy response of each silicon strip was first calibrated with an α-emitting radioactive source ^{244}Cm (5.805 MeV). Proton beams at the energies of 4- and 7-MeV scattering off of a ^{197}Au target were also used for energy calibration. By assuming elastic scattering and the measured detector geometry, the energy offset of each analog-to-digital convertor (ADC) channel could be obtained as well.

The total energy of each identified proton was then processed event by event for reconstruction of the reaction vertex. From the conservation of energy and momentum, the energy of proton (E_p) was calculated as [17]

$$E_p^{1/2} = \frac{(m_X m_p E_b)^{1/2}\cos\theta \pm \left[m_X m_p E_b \cos^2\theta + (m_Y + m_p)(m_Y Q + (m_Y - m_X)E_b)\right]^{1/2}}{m_Y + m_p},$$

where E_b is the beam energy, Q is the reaction Q-value, m_p, m_X and m_Y are the masses of the proton, beam (^{19}F) and the heavy recoil from the reaction (^{22}Ne), respectively, and θ is the angle between the beam axis and the path of the detected proton. Since the solution with minus sign only appears at extremely low incident beam energies, the equation was solved for $\cos\theta$ using the plus sign:

$$\cos\theta = \frac{A}{\sqrt{E_b E_p}}\left[B^2 E_p - B\left(m_Y Q + \left(m_Y - m_X\right)E_b\right)\right].$$

Two reaction specific constants A and B are defined as

$$A = \frac{1}{2\left(m_Y + m_p\right)\sqrt{m_X m_p}},$$

$$B = m_Y + m_p.$$

An example of reconstructed angle versus calibrated proton energy plot is shown in Fig. 4, which was obtained at $E_{\text{beam}} = 12$ MeV. The right and left curves represent the events from the (α, p) and (α, p') channel of the reaction, respectively. The angles were then used to obtain the reaction vertex of each identified event. An example of the reconstructed reaction vertex obtained at two different beam energies ($E_x = 11.76$- and 11.82-MeV) for the excited state (α, p') channel is shown in Fig. 5. At these beam energies, an energy level in ^{23}Na located at $E_x = 12.485$ MeV ($E_{\text{c.m.}} = 2.020$ MeV) was populated.

The excitation functions for the ^{19}F$(\alpha, p)^{22}$Ne and ^{19}F$(\alpha, p')^{22}$Ne* reactions were then calculated by using the yield and the solid angle covered by SIDAR at each reaction vertex, the number of beam particles incident on the target during the run, and the number of target atoms deduced from the ^{4}He gas pressure. The results are shown in Fig. 6. The top and bottom panels show the excitation functions obtained at various beam energies for the ^{19}F$(\alpha, p')^{22}$Ne* and ^{19}F$(\alpha, p)^{22}$Ne reaction channels, respectively. Two energy levels in ^{23}Na located at $E_{\text{c.m.}} = 2020 \pm 3$ keV and 2075 ± 2 keV were observed in multiple beam energies, where the uncertainties represent the standard deviations of the excitation energy distributions obtained at 12 ($E_b = 11.61$-, 11.64-, 11.67-, 11.70-, 11.73-, 11.76-, 11.78-, 11.79-, 11.82-, 11.85-, 11.88-, and 11.88-MeV) and 7 ($E_b = 11.97$-, 12.00-, 12.03-, 12.06-, 12.09-, 12.12, 12.15-MeV) beam energies, respectively. The level at $E_{\text{c.m.}} = 1997$ keV was only observed at the beam energy of 11.55 MeV. Since the cross section of the (α, p) channel is about one order of magnitude lower than that of the (α, p') channel at this energy range, the 1997 keV level

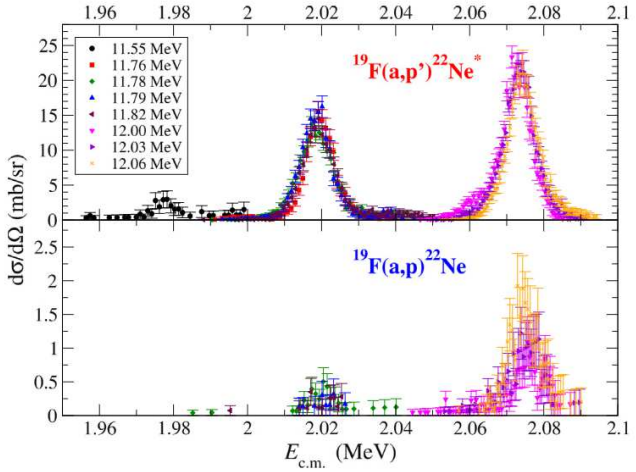

Fig. 6. (Color online) The excitation functions obtained at various beam energies for the $^{19}F(\alpha, p')^{22}Ne^*$ (top) and $^{19}F(\alpha, p)^{22}Ne$ (bottom) reactions are shown.

was not observed in the present $^{19}F(\alpha, p)^{22}Ne$ reaction channel. The contributions of natural line width, beam energy spread, and resolutions in energy and angle to the total widths of the peaks were estimated to be about 10 keV in the center of mass energy. Our results support those from the previous work by Cseh et al. [12], where the ^{23}Na energy levels were extensively studied by using α beams and a thick target method. In Ref. [12], many energy levels including the ones at $E_\alpha = 2.446$ and 2.515 MeV ($E_{c.m.} = 2.020$ and 2.077 MeV, respectively) were reported with uncertainties of about 3–5 keV.

The new technique will be used to measure astrophysically-important (α, p) reactions using radioactive beams at modern facilities. The $^{18}Ne(\alpha, p)^{21}Na$ reaction is an example. The reaction is believed to provide the breakout from the hot CNO cycles, fueling the *rp*-process [18]. Despite of many previous works on the $^{18}Ne(\alpha, p)^{21}Na$ reaction such as Refs. [4,19,20], the reaction rate at stellar temperature is still uncertain to some extent due to the lack of experimental data. By using this technique and short lived ^{18}Ne beams ($t_{1/2} = 1.672$ s), a better estimation of the astrophysical $^{18}Ne(\alpha, p)^{21}Na$ reaction rate can be obtained.

4. Conclusion

A new technique was developed to provide a sensitive approach for measuring astrophysical (α, p) reactions in inverse kinematics. A differentially pumped windowless gas target, gas recirculator, and large area silicon strip detector array were used to study the $^{19}F(\alpha, p)^{22}Ne$ and $^{19}F(\alpha, p')^{22}Ne^*$ reactions with low-energy ^{19}F beams. A newly developed gas recirculating system was used to reduce the gas consumption at the target chamber while keeping a very high purity of the target. Various beam energies in the range of $E_{beam} = 11.55$–12.12 MeV at the typical intensities of ~300 epA were used to bombard with the ^4He gas target kept at pressures of up to 9 Torr. Recoiling protons from the (α, p) and (α, p') reactions were detected by a silicon strip detector array located in the extended gas target chamber. By reconstructing the reaction vertex event-by-event, the excitation functions of the reactions could be obtained.

Two ^{23}Na energy levels located at $E_{c.m.} = 2020 \pm 3$ keV and 2075 ± 2 keV were observed from the present work, which shows good agreement with a previously reported study by Cseh et al. [12]. Since the viability of this technique is clearly shown through the present work, we are planning to apply this experimental method to measure astrophysically-important (α, p) reactions such as $^{18}Ne(\alpha, p)^{21}Na$ using radioactive heavy ion beams at modern accelerator facilities.

Acknowledgments

The authors wish to thank the staff members of the HRIBF for making this work possible. This work was supported by the National Research Foundation of Korea (NRF) grant funded by the Korea government (MEST) (No. NRF-2015R1D1A1A01056918, NRF-2016K1A3A7A09005579, and NRF-2016R1A5A1013277) and the US Department of Energy under Contract Nos. DE-AC05-00OR22725 (ORNL), DE-FG02-96ER40983 and DE-SC0001174 (University of Tennessee). This work was also supported by LG Yonam Foundation (of Korea).

References

[1] R.K. Wallace, S.E. Woosley, Astrophys. J. Suppl. 45 (1981) 389.
[2] R.E. Taam, Ann. Rev. Nucl. Part. Sci. 35 (1985) 1.
[3] H. Schatz, et al., Phys. Rev. Lett. 86 (2001) 3471.
[4] W. Bradfield-Smith, et al., Phys. Rev. C 59 (1999) 3402.
[5] A.A. Sonzogni, et al., Phys. Rev. Lett. 84 (2000) 1651.
[6] M. Notani, et al., Nuclear Phys. A 746 (2004) 113c.
[7] C. Fu, et al., Phys. Rev. C 76 (2007) 021603.
[8] V.Z. Goldberg, et al., Phys. Rev. C 69 (2004) 024602.
[9] D.K. Nauruzbayev, et al., Phys. Rev. C 96 (2017) 014322.
[10] B.H. Moazen, et al., Phys. Rev. C 75 (2007) 065801.
[11] J. Kuperus, Physica 31 (1965) 1603.
[12] J. Cseh, E. Koltay, Z. Mate, E. Somorjai, L. Zolnai, Nuclear Phys. A 413 (1984) 311.
[13] C. Ugalde, et al., Phys. Rev. C 77 (2008) 035801.
[14] J.R. Beene, et al., J. Phys. G 38 (2011) 024002.
[15] R.P. Fitzgerald, Measurement of the $^1H(^7Be,^8B)\gamma$ Cross Section (Ph. D. dissertation), University of North Carolina, 2005.
[16] D.W. Bardayan, et al., Phys. Rev. Lett. 83 (1999) 45.
[17] K.S. Krane, Nuclear reactions, in: Introductory Nuclear Physics, John Wiley & Sons, New Jersey, 1988, pp. 378–443.
[18] J.L. Fisker, E. Brown, M. Liebendörfer, H. Schatz, F.-K. Thielemann, Nucl. Phys. A 758 (2005) 447c.
[19] A.A. Chen, R. Lewis, K.B. Swartz, D.W. Visser, P.D. Parker, Phys. Rev. C 63 (2001) 065807.
[20] J.J. He, et al., Phys. Rev. C 88 (2013) 012801(R).